25th ABCM International Congress of Mechanical Engineering
October 20-25, 2019, Uberlândia, MG, Brazil

COBEM-2019-2037
NUMERICAL ANALYSIS OF A TRANSVERSAL CRACK MODEL FOR ROTATING FLEXIBLE SHAFTS

José Gustavo Campos Maruo
Izabela Batista da Silva
Aldemir Ap Cavalini Jr
Valder Steffen Jr
LMEst - Structural Mechanics Laboratory, Federal University of Uberlândia, School of Mechanical Engineering, Av. João Naves de Ávila, 2121, Uberlândia, MG, 38408-196, Brazil.
jose.maruo@ufu.br, izabela.silva@ufu.br, aacjunior@ufu.br, vsteffen@ufu.br

Abstract. *The crack presence in rotating machinery influences some mechanical properties, making necessary the inspection and monitoring of systems in order to avoid critical failures or accidents. The most common method of crack detection in rotating shafts is the vibration-based monitoring. This method can detect small changes in the physical features of the shafts like the crack presence, thanks to vibrational responses caused by local changes in the material flexibility. In this context, computational approaches are very useful to study the static behavior of cracked flexible shafts. The present paper aims to evaluate the effects of a transversal crack with different depths in two shaft-bearing-disc numerical models. A 1D finite element model of the shaft with an open crack is used, as well as a 3D non-linear model formulated at the same conditions.*

Keywords: *transversal cracks, static analysis, 1D and 2D finite element models.*

1. INTRODUCTION

The presence of cracks in shafts stands as one of the most dangerous and critical faults in rotating machines, which can lead to long periods of downtime and several economic consequences (Ferreira, 2010). A crack may propagate from some small imperfections on the surface of the body or inside of the material and it is most likely to appear in correspondence of high-stress concentration, thus its direction of propagation and propagation speed as a function of the stress level are problems to which many studies have been dedicated in the last 50 years (Bachschmid et al.,2010). Muszynska (2005) states that crack detection in its initial phase and the prediction of its behavior can avoid unnecessary failures and downtimes of a system.

Structural Health Monitoring (SHM) techniques are used for damage detection in aerospace, civil, and mechanical engineering systems. The SHM techniques involve the observation of a system over time, among the extraction of damage-sensitive features and their statistical analysis to determine the current state of the system (Farrar, 2005). Considering that the presence of defects causes typical excitations, vibration measurement monitoring can be considered an SHM that allows a real-time preventive inspection, enabling error identification before failures and accidents, providing better planning and maintenance (Ferreira, 2010).

The influence of transversal cracks on mechanical properties of rotating shafts is a topic covered mainly by literature. Many authors proposed different mathematical models to represent the static and dynamic behavior of a cracked rotating shaft. Crack breathing behavior is showed in Gasch (1976), Mayes and Davies (1984), and Bachschmid et al. (2010), while AL-shudeifat (2013) proposed an open crack model based on the advanced phase of breathing crack

According to Dimarogonas (1996) and Bachschmid et al. (2010), the presence of a crack in a structure introduces local flexibility that affects its vibrational response. Still, according to Dimarogonas (1996), the linear fracture mechanics theory can be used together with the strain energy release rate, the stress intensification factors, and the Castiglione theorem to calculate the local flexibility of the crack region, as well as the associated stiffness variation.

In this context, the present paper aims to study the influence of transversal cracks in the static behavior of flexible shafts by using the 1D and 3D finite element models formulated in MATLAB® and ANSYS®, respectively. For this purpose, a shaft-bearing-disc system is used. For the 1D model, the crack was included in the shaft using the additional flexibility matrix proposed by Papadopoulos and Dimarogonas (1987). For the 3D model, the crack was simulated with a cut on the cross-section of the shaft. The crack is considered always open, independently of the shaft angular position. The analysis covered from 0 to 50% crack depths, with steps of 5% (with percentage relative to the shaft diameter). Finally, a comparison with the numerical analysis developed by Silva (2017, 2018) is presented.

2. NUMERICAL MODEL

Following the test rig used by Silva (2017, 2018), the 1D and 3D finite element models were constructed based on a shaft-bearing-disc system composed of a flexible steel shaft with 1005 mm length and 17 mm diameter (E = 205 GPa, ρ = 7850 kg/m^3, ν = 0.29), one rigid steel disc with 150 mm diameter and 20 mm thickness (ρ = 7850 kg/m3), and two ball bearings.

2.1 1D Model

The 1D finite element model was developed in MATLAB® as in Silva (2017, 2018), and it was formulated based on Timoshenko's beam theory, assuming that the shaft is flexible and the disc is rigid. The considered shaft element with two nodes and four freedom degrees per node (*u, W, θ, φ*) is shown in Fig. 1.

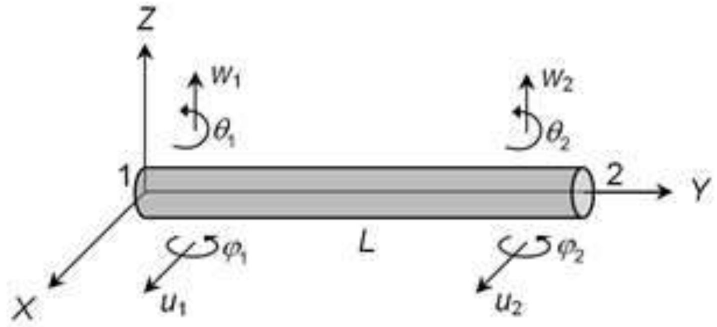

Figure 1. Timoshenko beam element with 8 degrees of freedom, Cavalini Jr.(2013).

Figure 2 shows the shaft-bearing-disc system formulated with 38 beam elements. The crack is assumed to be at element #14 (between nodes #14 and #15). The two ball bearings are located at the nodes #2 and #6. The disc is located at node #37.

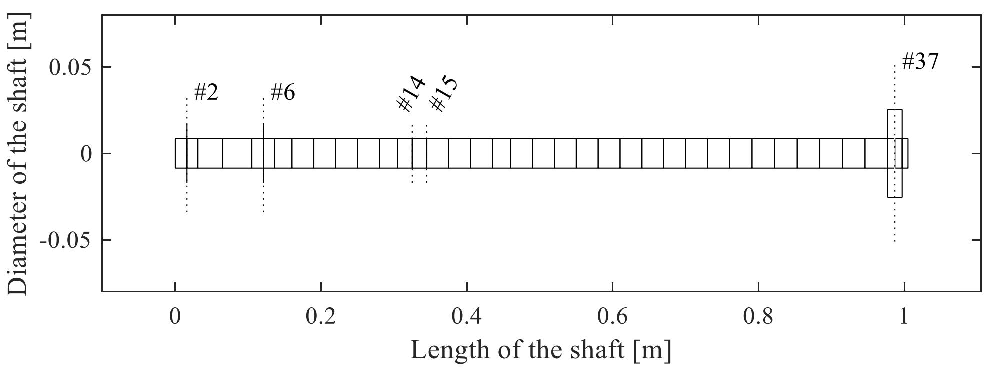

Figure 2. Shaft-bearing-disc finite element model, Silva(2017).

The dynamic behavior of cracked flexible shaft supported by ball bearings is mathematically presented in Eq. (1).

$$\boldsymbol{M}\ddot{\boldsymbol{q}} + \boldsymbol{D}\dot{\boldsymbol{q}} + \boldsymbol{K}\left(\Omega t\right)\boldsymbol{q} = \boldsymbol{W} \tag{1}$$

where ***M*** is the mass matrix, ***D*** is the damping matrix, ***K(Ωt)*** is the stiffness matrix with variable values due to the crack (i.e., *Ωt* stands to the angular position of the shaft), ***W*** stands for the weight of the rotating parts, and ***q*** is the generalized displacement vector.

The dynamic model of the finite shaft element with a crack is obtained first using the linear fracture mechanics theory to determine the additional flexibility produced by the crack, assuming a beam element with diameter *D* containing a transverse crack with depth *α*, as in Fig. 3.

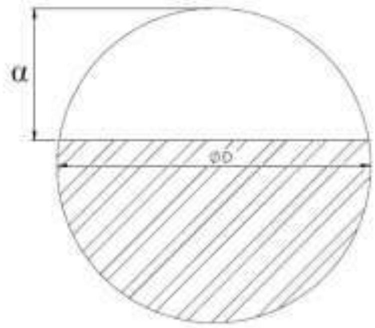

Figure 3. Cross-section of a crack element. The crack appears as the region without hatching.

The Castiglione theorem determines the cracked shaft displacement q_i in the direction of the load P_i, as presents the Eq. (2) (Darpe *et al.*, 2004).

$$q_i = \frac{dU}{dP_i} = \frac{\partial U^0}{\partial P_i} + \frac{\partial U^c}{\partial P_i} \tag{2}$$

where U^0 is the elastic strain energy of the shaft element with crack, as in Eq. (7) in Darpe *et al.* (2004), and U^c is the additional strain energy due to the crack presence, shown in Eq (3).

$$U^c = \int_A J(A)\,dA = \int_A \frac{1-\upsilon}{E}\left[\left(\sum_{i=1}^{6} K_{Ii}\right)^2 + \left(\sum_{i=1}^{6} K_{IIi}\right)^2 + (1+\upsilon)\left(\sum_{i=1}^{6} K_{IIIi}\right)^2\right] \tag{3}$$

where E is Young's modulus, v is the Poisson's ratio, G is the shear modulus, I represents the area moment of inertia, and I_0, the polar moment of inertia. K_{Ii}, K_{IIi}, and K_{IIIi} are the stress intensity factors (SIF). In this case, the principal load is applied normal to the crack plane; therefore, only the crack load mode K_{Ii} is considered (Anderson, 2005). The SIF are shown in Eq. (4).

$$K_{mi} = Y\sigma_i\sqrt{\pi\alpha} \tag{4}$$

where K_{mi} is the SIF (I, II or III), σ_i is the stress distribution on the crack, and Y are the shape functions. The additional flexibility c_{ij} is obtained as exposed in Eq. (5).

$$c_{ij} = \frac{\partial^2 U^c}{\partial P_i \partial P_j} \tag{5}$$

where the resulting integrals were calculated by using the procedure described in Papadopoulos (2004). Thus, the additional flexibility matrix due to the crack is given by the Eq. (6).

$$\boldsymbol{c} = \begin{bmatrix} 0 & 0 & 0 & 0 \\ & 0 & 0 & 0 \\ & & c_{55} & c_{56} \\ sim. & & & c_{66} \end{bmatrix} \tag{6}$$

The additional flexibility matrix due to the crack is then added to the flexibility matrix of the uncracked shaft ($\boldsymbol{c_0}$) to obtain the resulting flexibility of the shaft element with the crack, as in Eq. (7).

$$\boldsymbol{c_{CE}} = \boldsymbol{c_0} + \boldsymbol{c} \tag{7}$$

Equation (8) presents the stiffness coefficients k_ξ and k_η that are obtained from the inverse value of $\boldsymbol{c_{CE}}$ ($k_\xi = \boldsymbol{c_{CE}}^{-1}(1,1)$, $k_\eta = \boldsymbol{c_{CE}}^{-1}(2,2)$), which are used for determining the stiffness of the cracked shaft in fixed coordinates $\boldsymbol{K_F}$, that changes according to the angular position of the shaft.

$$\boldsymbol{K_F} = \begin{bmatrix} cos(\theta) & -sin(\theta) \\ sin(\theta) & cos(\theta) \end{bmatrix} \begin{bmatrix} k_\xi & 0 \\ 0 & k_\eta \end{bmatrix} \begin{bmatrix} cos(\theta) & sin(\theta) \\ -sin(\theta) & cos(\theta) \end{bmatrix} \tag{8}$$

where θ is the angular position of the shaft ($\theta = \Omega t$).

Finally, the stiffness matrix of the shaft element with the transverse crack $\boldsymbol{K_{CE}}$ is calculated by a combination of the matrices shown in Eq. (9) and Eq. (10) as follows:

$$\boldsymbol{K_{XY}} = \frac{12EI}{L^3(1+\vartheta_Y)} \begin{bmatrix} -1 & 0 \\ L & -1 \\ 1 & 0 \\ 0 & 1 \end{bmatrix} \begin{bmatrix} K_F(1,1) & \frac{L}{2} \\ \frac{L}{2} & \frac{(4+\vartheta_Y)}{12}L^2 \end{bmatrix} \begin{bmatrix} -1 & L & 1 & 0 \\ 0 & -1 & 0 & 1 \end{bmatrix} \tag{9}$$

$$\boldsymbol{K_{YZ}} = \frac{12EI}{L^3(1+\vartheta_Y)} \begin{bmatrix} -1 & 0 \\ -L & -1 \\ 1 & 0 \\ 0 & 1 \end{bmatrix} \begin{bmatrix} K_F(2,2) & -\frac{L}{2} \\ -\frac{L}{2} & \frac{(4+\vartheta_Y)}{12}L^2 \end{bmatrix} \begin{bmatrix} -1 & -L & 1 & 0 \\ 0 & -1 & 0 & 1 \end{bmatrix} \tag{10}$$

2.2 3D Model

Figure 4 shows the 3D model of the shat-bearing-disc developed by using the software ANSYS®, according to the geometry and parameters already presented in this work.

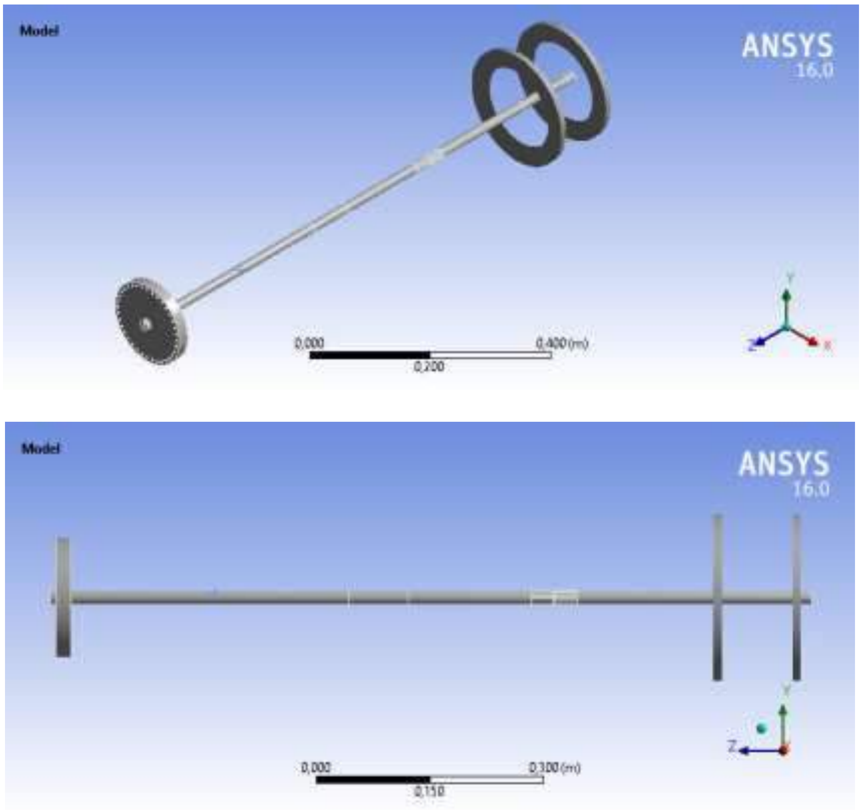

Figure 4. 3D model developed in Ansys®.

The bearings are represented by two connections *Ground to Multiple*, and a cross-section cut represents the crack. The mesh was created by the sweep method with solid hexahedral and tetrahedral elements. A refinement was used in the crack region, considering a 1 mm element size for representativeness purposes, as shown in Fig. 5.

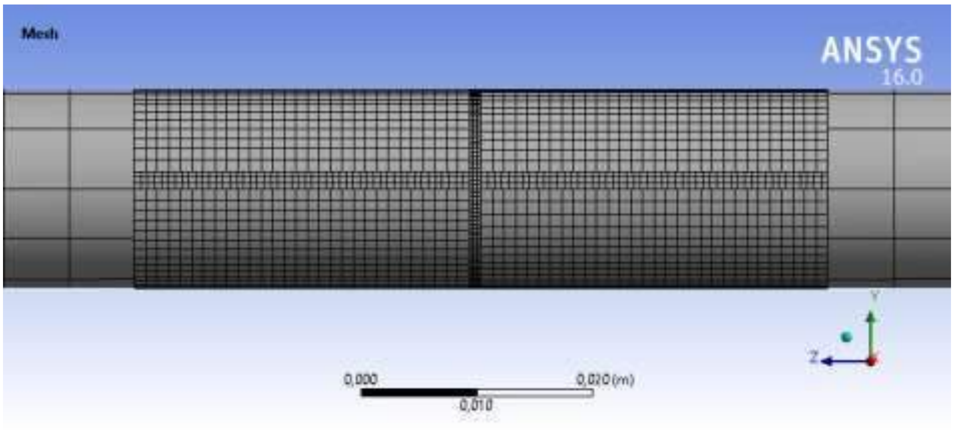

Figure 5. Mesh refinement in the crack region, for the shaft without cracking.

The total number of elements for each crack depth can be visualized in Tab. 1.

Table 1. Number of elements for discretization of each crack depth.

Crack Depth (%)	0	5	10	15	20	25	30	35	40	45	50
Number of elements	29573	28983	29043	28908	27801	28278	27909	27564	27189	27135	26331

The analysis were made by using the static structural solution with five probes (1 to 4 positioned at 310 mm, and 5 positioned at 340 mm from the first bearing) that were used to measure the strain fields near to the crack location and around the shaft, as shown in Fig. 6.

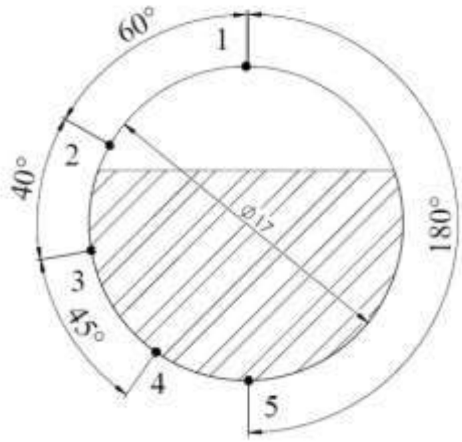

Figure 6. Positions of the probes around the shaft, for an arbitrary crack depth.

3. RESULTS

To facilitate the comparison between the results of the 1D and 3D models, the strain values (µS) are shown in a fit curve as a function of the shaft angular position (°) for each crack depth. The fit curve was calculated through the least-squares method considering a sixth-degree polynomial. The results are organized in 5 figures (Fig. 7 to Fig. 11), where each one represents a specific probe (1 to 5). It is possible to observe that these graphics have a mainly qualitative featuring.

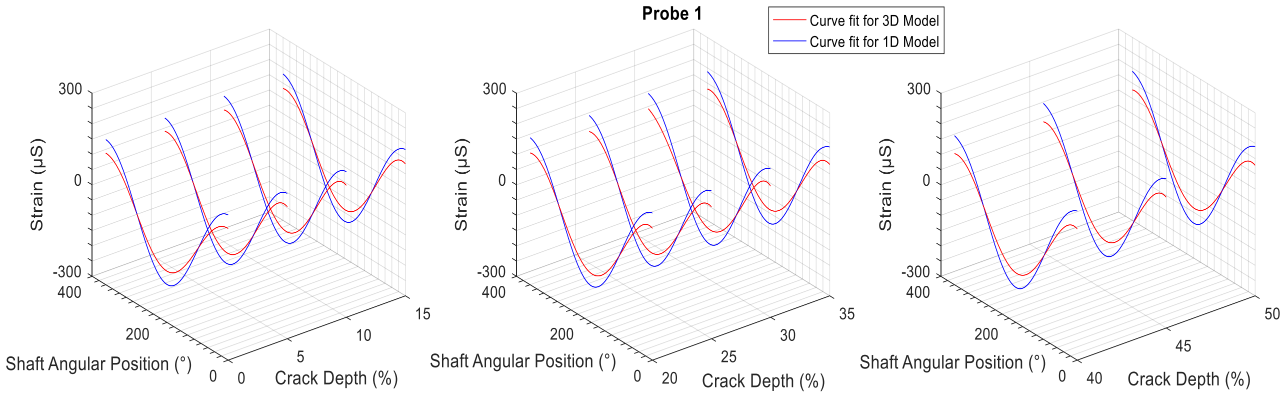

Figure 7. Strain as a function of the shaft angular position for Probe 1.

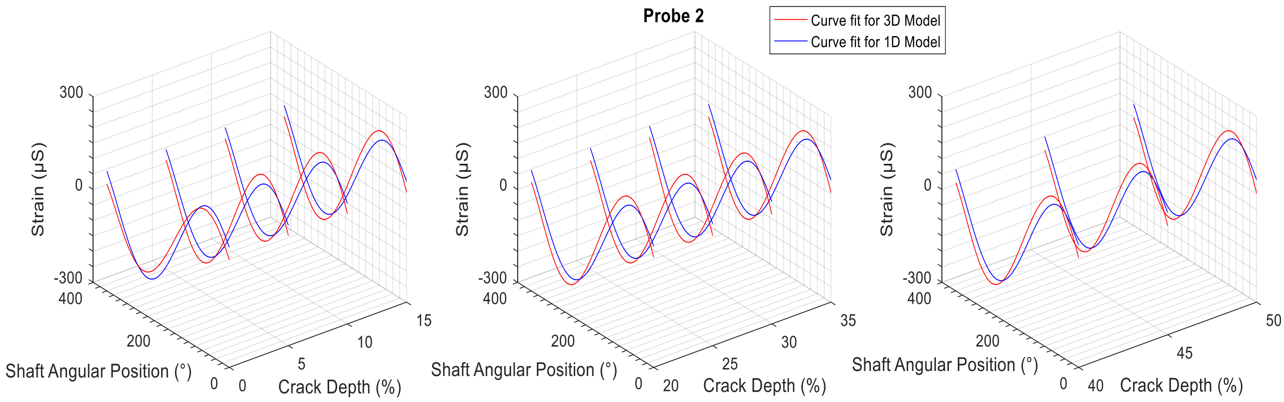

Figure 8. Strain as a function of the shaft angular position for Probe 2.

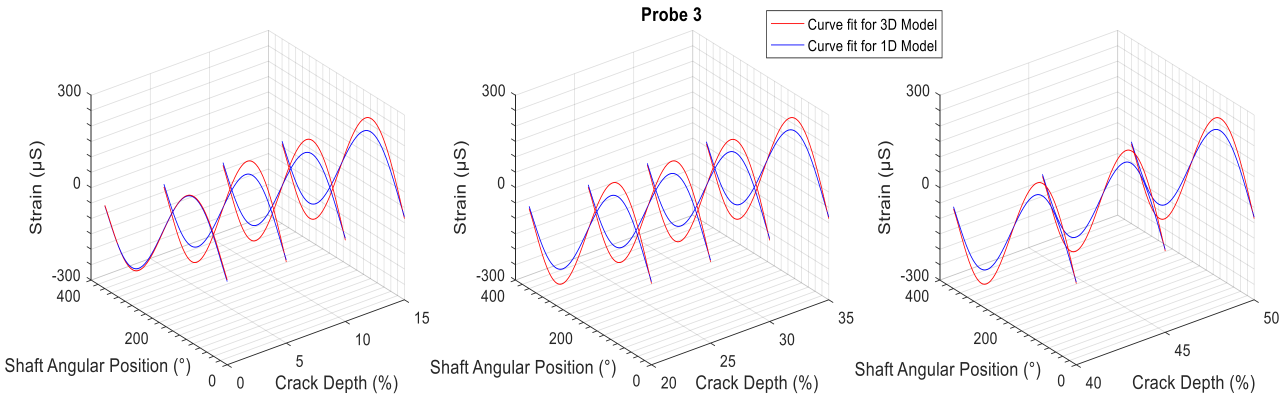

Figure 9. Strain as a function of the shaft angular position for Probe 3.

Note that the strain curves follow a similar shape between the models. Most of the strain values obtained have the same range (-300 to 300 μS), except for the deeper crack in the probe 5 (3D model), where the stain values were increased (-490 to 490 μS).

This work has been partially presented by Silva (2017, 2018), which showed graphics for strain values as a function of angular position for cracks with 0%, 20%, and 50% depth, comparing 1D and 3D models, including also experimental results.

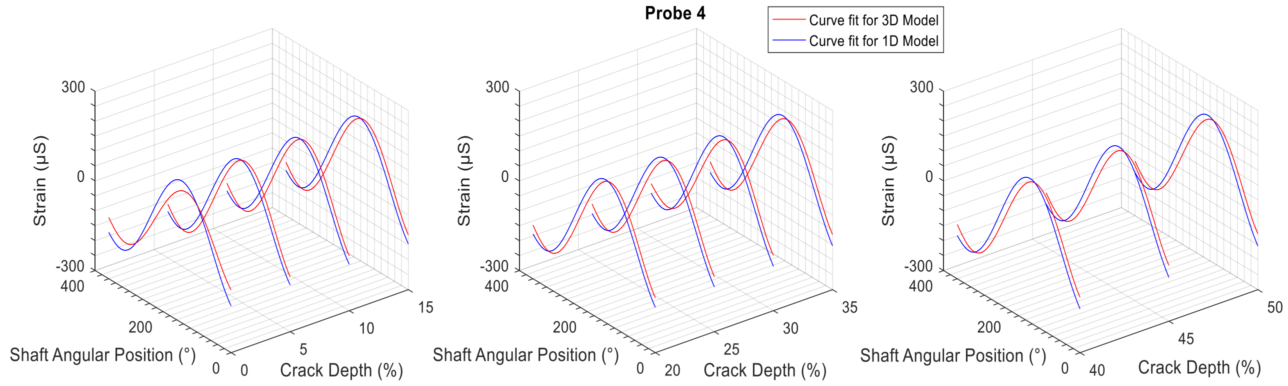

Figure 10. Strain as a function of the shaft angular position for Probe 4.

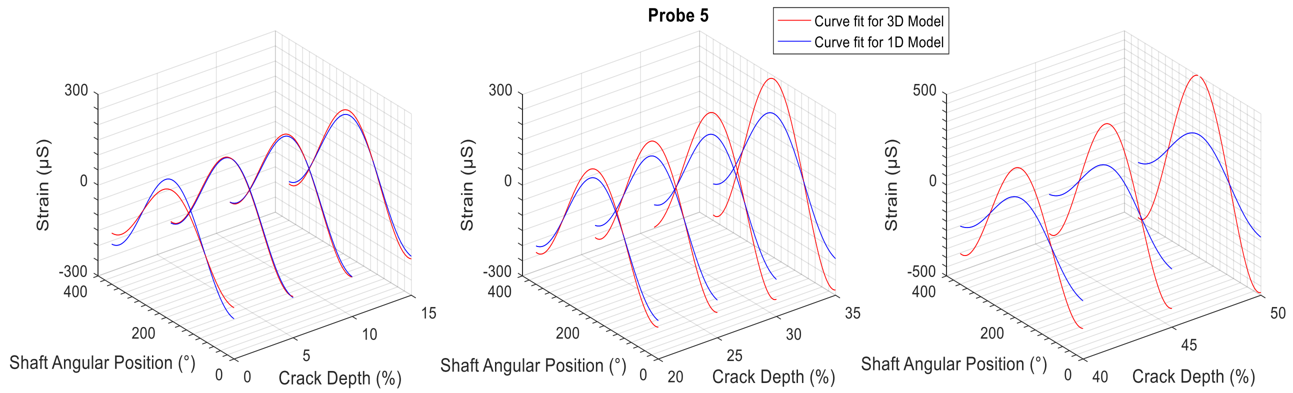

Figure 11. Strain as a function of the shaft angular position for Probe 5.

4. CONCLUSIONS

In the present contribution, 1D and 3D finite element models formulated in MATLAB® and ANSYS® respectively were constructed for static comparison of the flexible cracked shaft. A system composed of a shaft-bearing-disc was used for this purpose. The crack was simulated according to a fully open model. The strain field at five locations along the shaft was measured for different depth crack and different angular positions. The results obtained by using both models demonstrated to be similar in most studied cases.

In probe 5 (located opposite of the crack), the divergence between the models for deeper cracks (Fig. 11) can be justified by the fact that the 1D model does not predict nonlinear behavior. As future works, the crack element size of the models will be optimized as a function of the depth crack.

5. ACKNOWLEDGMENTS

The authors are thankful for the financial support provided to the present research effort by CNPq (574001/2008-5,304546/2018-8, and 431337/2018-7), FAPEMIG (TEC-APQ-3076-09, TEC-APQ-02284-15, TEC-APQ-00464-16, and PPM-00187-18), and CAPES through the INCT-EIE.

6. REFERENCES

Al-Shudeifat, M. A., 2013. *On the finite element modeling of the asymmetric cracked rotor*. Journal of Sound and Vibration.

Anderson, T. L., 2005. *Fracture Mechanics: Fundamentals and Applications*, Taylor & Francis, USA.

Bachschmid, N.; Pennacchi, P. and Tanzi, E., 2010. *Cracked rotors: a survey on static and dynamic behavior including modeling and diagnosis*, Springer

Cavalini Jr., A. A., 2013. *Detecção e Identificação de Trincas Transversais Incipientes em Eixos Horizontais Flexíveis de Máquinas Rotativas*. Doctoral thesis, Universidade Federal de Uberlândia, Uberlândia, Brasil.

Darpe, A.K.; Gupta, K. and Chawla A., 2004. *Coupled bending, longitudinal and torsional vibrations of a cracked rotor*. Journal of Sound and Vibration, Vol. 269, n. 1, p. 33-60.

Dimarogonas, A.D., 1996. *Vibration of cracked structures: a state of the art review.* Engineering Fracture Mechanics. Vol. 55, n. 5, p. 831-857.

Farrar, C.R.; Lieven, N.A.J. and Bement, M.T., 2005. "An Introduction to Damage Prognosis". In: Inman, D.J.; Farrar, C.R.; Lopes, V. and Steffen, V. (Eds.). *Damage Prognosis: For Aerospace, Civil and Mechanical Systems*, John Wiley & Sons Ltd, England, p. 1-12.

Ferreira, B. F., 2010. *Detecção de Trincas em Eixos Rotativos Através de Medição de Vibrações*. Masters thesis, Universidade de Brasília, Brasília, Brasil.

Gasch, R., 1976. Dynamic behaviour of a simple rotor with a cross sectional crack. In: *International Conference on Vibrations in Rotating Machinery*, IMechE, Vol. 1, n. 1, p. 123-128.

Mayes, I.W. and Davies, W.G.R., 1984. *Analysis of the response of multi-rotor-bearing system containing a transverse crack in a rotor*. Journal of Vibration, Acoustics, Stress, and Reliability in Design, Vol. 106, n. 1, p. 139-145.

Muszynska, A., 2005. *Rotordynamics*, Taylor & Francis Group.

Papadopoulos, C.A., 2004. *Some comments on the calculation of the local flexibility of cracked shafts*. Journal of Sound and Vibration, Vol. 278, n. 1, pp. 1205–1211.

Papadopoulos, C.A. and Dimarogonas, A.D., 1987. *Coupled longitudinal and bending vibrations of a rotating shaft with an open crack*. Journal of Sound and Vibration, Vol. 117, n. 1, p. 81-93.

Silva, I. B. da., 2018. *Análise da influência de trincas transversais no comportamento estático e dinâmico de eixos flexíveis.* Masters thesis, Universidade Federal de Uberlândia, Uberlândia, Brasil.

Silva, I. B. da., 2017. "Numerical and experimental analysis of a cracked shaft based on static and dynamic responses". In *Proceedings of the 24th International Congress of Mechanical Engineering - COBEM 2017*. Curitiba, Brazil.

7. RESPONSIBILITY NOTICE

The authors are the only responsible for the printed material included in this paper.